ARTICLES

Journal of Semiconductors
(2020) 41, 042602
doi: 10.1088/1674-4926/41/4/042602

Growth of aligned SnS nanowire arrays for near infrared photodetectors

Guozhen Shen[1, 2, †], Haoran Chen[1, 2], and Zheng Lou[1]

[1]State Key Laboratory for Superlattices and Microstructures, Institute of Semiconductors, Chinese Academy of Sciences, Beijing 100083, China
[2]Center of Materials Science and Optoelectronic Engineering, University of Chinese Academy of Sciences, Beijing 100049, China

Abstract: Aligned SnS nanowires arrays were grown via a simple chemical vapor deposition method. As-synthesized SnS nanowires are single crystals grown along the [111] direction. The single SnS nanowire based device showed excellent response to near infrared lights with good responsivity of 267.9 A/W, high external quantum efficiency of 3.12×10^4 % and fast response time. Photodetectors were built on the aligned SnS nanowire arrays, exhibiting a light on/off ratio of 3.6, and the response and decay time of 4.5 and 0.7 s, respectively, to 1064 nm light illumination.

Key words: photodetectors; nanowires; infrared; aligned

Citation: G Z Shen, H R Chen, and Z Lou, Growth of aligned SnS nanowire arrays for near infrared photodetectors[J]. *J. Semicond.*, 2020, 41(4), 042602. http://doi.org/10.1088/1674-4926/41/4/042602

1. Introduction

Orthorhombic tin sulfide (SnS) is an important member of anisotropic layered IV–VI group semiconductors, where Sn atoms are coordinated to three S atoms to form the puckered Sn–S layers coupled by weak van der Waals forces[1, 2]. The mid near infrared (NIR) direct band gap of 1.3 eV and high absorption coefficient larger than 10^4 cm^{-1} make SnS an ideal candidate for NIR photodetectors[3–5]. Due to the high specific surface area and the confinement of charge carriers, one-dimensional (1D) or two-dimensional (2D) SnS nanostructures exhibited obvious advantages compared with the thin film or nanoparticle counterparts[6–10]. For example, SnS nanobelts from solution method showed a responsivity of 3 μA/(W·cm). SnS nanobelts from vapor-based method exhibited excellent photoresponsivity of 300 A/W under 800 nm light. SnS nanosheets showed obvious anisotroic photoresponse with a photoresponsivity of 365 A/W to 808 nm light and the performance can be further improved by Au nanoparticles decoration.

Nanowire (NW) arrays have the characteristics of large effective irradiation area, the multiple scattering of incident light, and the increased path length of incident light. Using NW arrays to trap light provides an effective way to improve the absorption capacity of photoelectric devices[11–15]. For example, Jie *et al*. demonstrated ZnO–MoS_2 core–shell nanopillar arrays based broadband ultraviolet-visible-near infrared photodetectors[11]. They found that the photocurrent is improved by up to 60 times compared with the planar heterojunctions. Fan *et al*. developed a template-guided vapor phase method to grow $CH_3NH_3PbI_3$ ($MAPbI_3$) NW arrays with unprecedented control of NW diameter from the bulk (250 nm) to the quantum confined regime (5.7 nm)[12]. This strategy enabled a 56-fold increase in internal photoluminescence quantum yield, and 2.3-fold increase in out-coupling efficiency. Moreover, their group also achieved an impressive optimal absorption efficiency (~99%) by tuning the highly ordered Ge nanopillar arrays through shape and geometry control[14]. As a result, it is also expected that the light-absorbing ability of SnS NWs can be remarkably improved by using NW arrays, giving high performance NIR photodetectors.

In this work, we report the preparation of aligned SnS NW arrays using chemical vapor deposition method. As-grown individual SnS NW exhibited excellent response to near infrared lights with good responsivity of 267.9 A/W, high external quantum efficiency of 3.12×10^4 % and fast response time. Photodetectors constructed from the aligned SnS NW arrays were demonstrated to be capable to detect NIR lights (808–1450 nm) with the photocurrent enhanced about 5 times compared with single NW.

2. Experimental

Aligned SnS NW arrays were synthesized via a simple chemical vapor deposition method. In a typical process, high purity SnS powders (99.5%, Alfa) were put into a ceramic boat, which was placed in the center of a quartz tube of a tube furnace. The silicon substrate covered with a thin layer of Au film (10 nm) was placed at the downstream about 1–2 cm away from the boat. The furnace was first purged with high purity Ar gas for 30 min and then heated to 750 °C and kept at that temperature for 30 min. After cooling down to room temperature, a layer of black powders was found deposited on the whole substrate.

The prepared samples were characterized using scanning electron microscope (SEM, FEI NanoSEM650), transmission electron microscope (TEM, JEM-2100F) equipped with an X-ray energy dispersive spectrometer (EDS) and X-ray diffractometry (XRD, Rigaku D/Max-2550).

To investigate the optoelectronic properties, the as-grown SnS nanowires were dispersed into isopropanol (IPA) and dropped onto SiO_2/Si substrates. Standard photolitho-

Correspondence to: G Z Shen, gzshen@semi.ac.cn
Received 5 MARCH 2020; Revised 10 MARCH 2020.

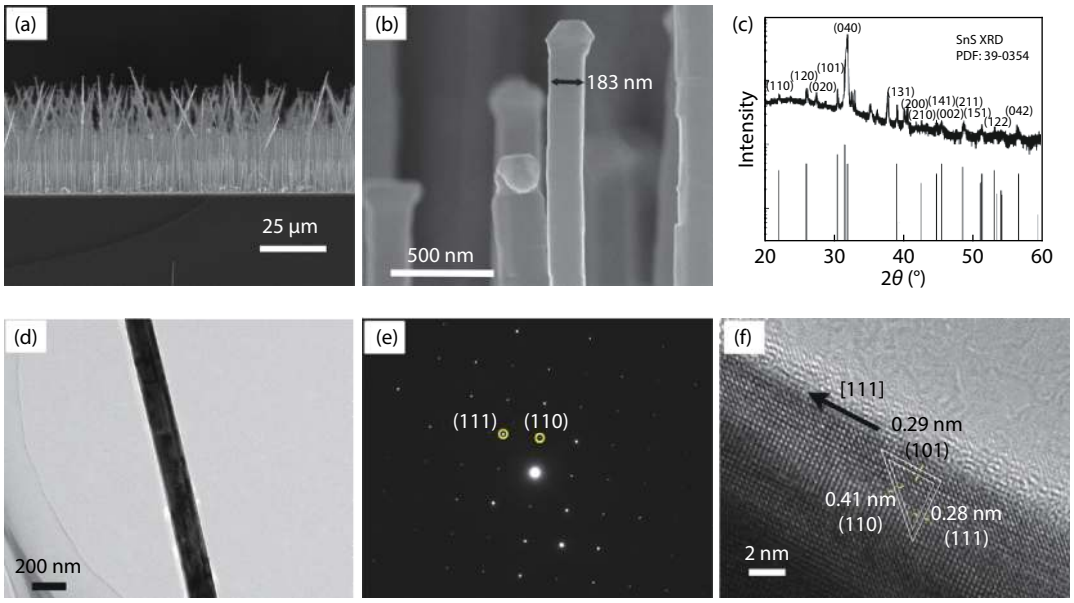

Fig. 1. (Color online) (a, b) SEM images, (c) XRD pattern, (d) TEM image, (e) SAED pattern and (f) HRTEM image of the synthesized SnS nanowires.

graphy was then performed to pattern the electrode. 100 nm Au was then deposited on the terminals of a single SnS NW as the source and drain electrodes. The corresponding measurements were carried out with a probe station connected with a Keysight B1500A semiconductor characterization system. Near infrared lasers with different wavelengths and tunable light intensities were adopted as the illumination source. All measurements were carried out in air at room temperature.

3. Results and discussions

Fig. 1(a) showed the cross-section view SEM image of the sample deposited on Si substrate. High density nanowires were found aligned on the substrate, forming into aligned NW arrays. Typical NWs have the diameters ranging from 100 to 300 nm. High-resolution SEM image of a single NW was shown in Fig. 1(b), where the NW has a diameter of 183 nm with smooth surface. Nanoparticle was found on top of the NW, indicating typical vapor–liquid–solid (VLS) growth mechanism[16–20]. To get information about the composition of the NWs, XRD was carried out and the corresponding XRD pattern was shown in Fig. 1(c). All the typical peaks in this pattern can be readily indexed to pure SnS with the orthorhombic phase (JCPSD card, No. 39-0354). TEM was then performed to get information about the microstructure of the SnS NW. A TEM image of an individual SnS NW is depicted in Fig. 1(d), in consistent with the SEM result. The corresponding selected-area electron diffraction (SAED) pattern in Fig. 1(e) indicated the single-crystalline nature of the SnS NW. Fig. 1(f) gave the high-resolution TEM (HRTEM) image of the SnS NW. The clearly resolved lattice fringes were 0.29, 0.41, and 0.28 nm, corresponding to the (101), (110), and (111) planes of orthorhombic SnS phase, respectively. Based on the above results, it confirmed that single crystalline SnS NWs along the [111] directions were successfully synthesized in the present work.

To study the photoresponse properties of the synthesized SnS sample, single NW device was first fabricated via a conventional photolithography and lift-off process, according to our previous reports[21–24]. Fig. 2(a) showed the SEM image of the fabricated single NW device, where the NW was found gated by two electrodes. The channel width of the device is around 5 μm. The I–V characteristics of the device measured at room temperature in dark and with NIR light illumination (808, 915, 1064, 1342 nm) were depicted in Fig. 2(b). It can be seen that the photocurrent increased sharply when the device was exposed to light irradiation. Besides, the devices showed obvious response to all the given light irradiation, confirming the NIR detection ability room temperature. The current versus voltage curves of the device to 1064 nm light irradiation at various light intensities as well as the dark current were demonstrated in Fig. 2(c). With increased light intensities, the photocurrents gradually increased. The relationship between photocurrent and light intensity of the device was shown in Fig. 2(d), following a power law of $\Delta I \sim 9.4 \times P^{0.44}$. It meant that the increase of photocurrent would be gradually slowed down with enhanced P[25–27]. Dynamic photoresponse performance of the device to 1064 nm NIR light with the light intensity of 8.1 mW/cm^2 was shown in Fig. 2(e). The photocurrents versus time curves were recorded at 3 V bias by periodically turning the NIR light on and off. From the curves, we can see that the photocurrent increased sharply and was stable at the saturated state when the light was turned on. While it immediately decreased and recovered to its initial state once the light was turned off. Over the six test cycles, there is no obvious decay of the photocurrent upon turning on/off the light periodically, implying a good reproducibility and stability of the device to NIR light irradiation.

Response time and decay time are the key parameters to measure the response speed of a photodetector. Generally, the response time is defined as the time taken for the current of the device to increase from 10% to 90% of the peak value, while the decay time is defined to be the opposite[27]. Fig. 2(f) showed the response time and recover time curve of the device, which were measured to be 0.22 and 1.42 s, respectively, comparable to some of the previous reported data[8–10].

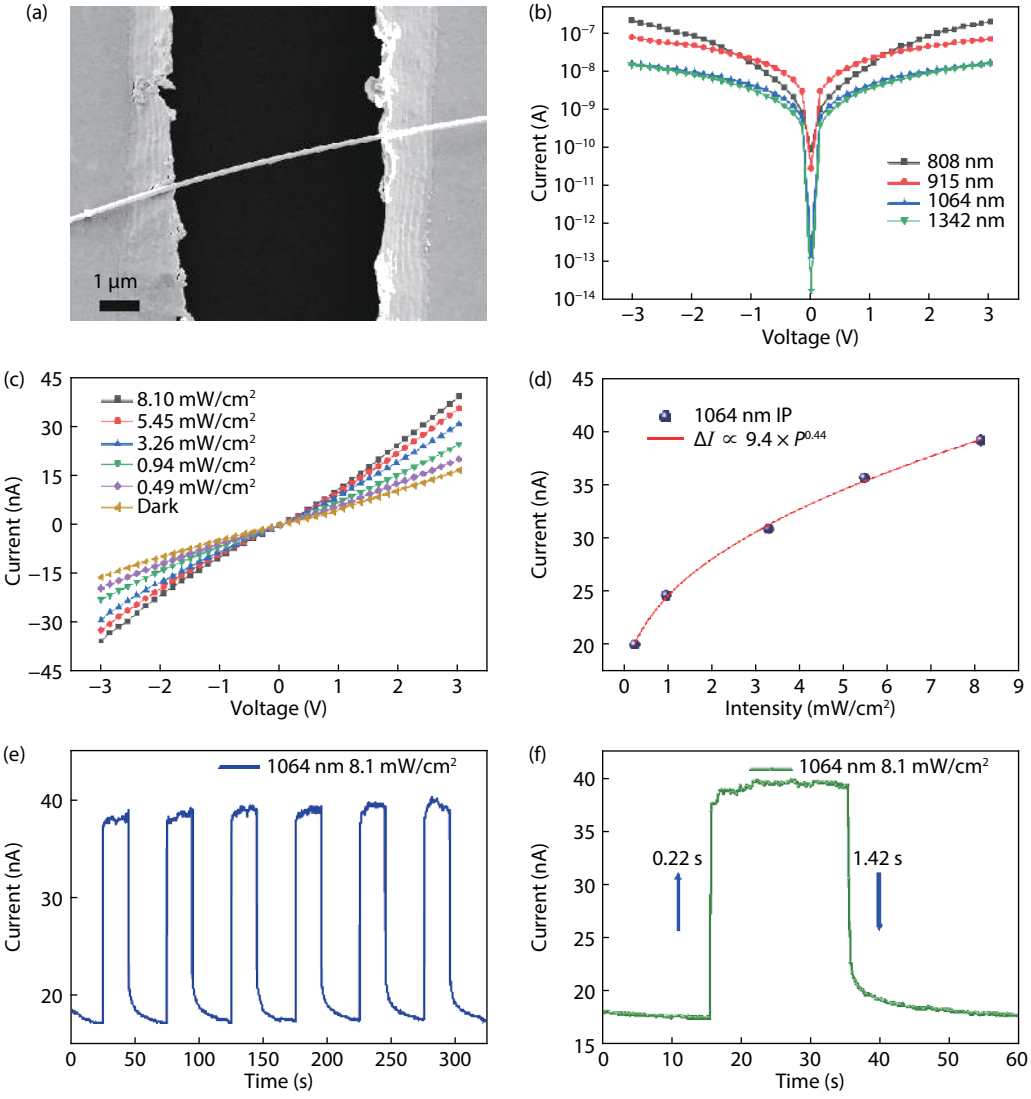

Fig. 2. (Color online) Characterizations of the single SnS nanowire based photodetector. (a) SEM image of a single nanowire device. (b) *I*–*V* curves of the device to NIR lights of 808, 915, 1064 and 1342 nm, respectively. (c) *I*–*V* curves of the device to 1064 nm lights with different light intensities. (d) Light intensity dependent photocurrent at a fixed bias voltage of 3 V. (e) The reproducible and stable switching behavior of the device to 1064 nm light. (f) Transient response and decay time of the device.

The responsivity (R_λ) and the external quantum efficiency (EQE) are important parameters to evaluate a photodetector. They can be defined as[27–29]:

$$R_\lambda = \frac{\Delta I}{PS} = \frac{I_{\text{photo}} - I_{\text{dark}}}{PS}, \tag{1}$$

$$\text{EQE} = R_\lambda \frac{hc}{e\lambda}. \tag{2}$$

In these equations, P is the power intensity of the incident light, S is the effective illumination area, I_{photo} and I_{dark} are the photo current and the dark current, h is the Planck's constant, c is the velocity of incident light, e is the elementary electronic charge, and λ is the wavelength of incident light. According to these equations, under 1064 nm light illumination with the light intensity of 8.1 mW/cm^2, the responsivity and EQE are calculated to be 267.9 A/W and 3.12 × 10^4 %, respectively. The specific detectivity (D^*) is another important parameter for a photodetector, which can be defined as follows[27]:

$$D^* = R_\lambda \left(\frac{S\Delta f}{2eI_{\text{dark}}} \right)^{1/2}, \tag{3}$$

where R_λ is responsivity, and Δf is the band width. From the data in Fig. 2, the D^* was calculated to be around 3.63 × 10^{11} J.

As the synthesized SnS NWs exhibited excellent photoresponse to NIR illumination, we then fabricated photodetectors based on the aligned SnS NW arrays. Fig. 3(a) demonstrated the schematic illustration of the typical fabrication process. Briefly, silicon substrate was coated with a layer of Au film to grow the aligned SnS NW arrays. After the growth, a layer of polymethyl methacrylate (PMMA) was spin-coated on the NW arrays. Silver NWs were then coated on the PMMA layer, acting as one electrode of the device. In this structure, PMMA was used to avoid the direct contact of Ag NWs with Si, another electrode of the device. The corresponding SEM images of the devices were shown in Figs. 3(b) and 3(c), clearly illustrating the coating of Ag NWs and PMMA on the SnS NW arrays (marked with arrows).

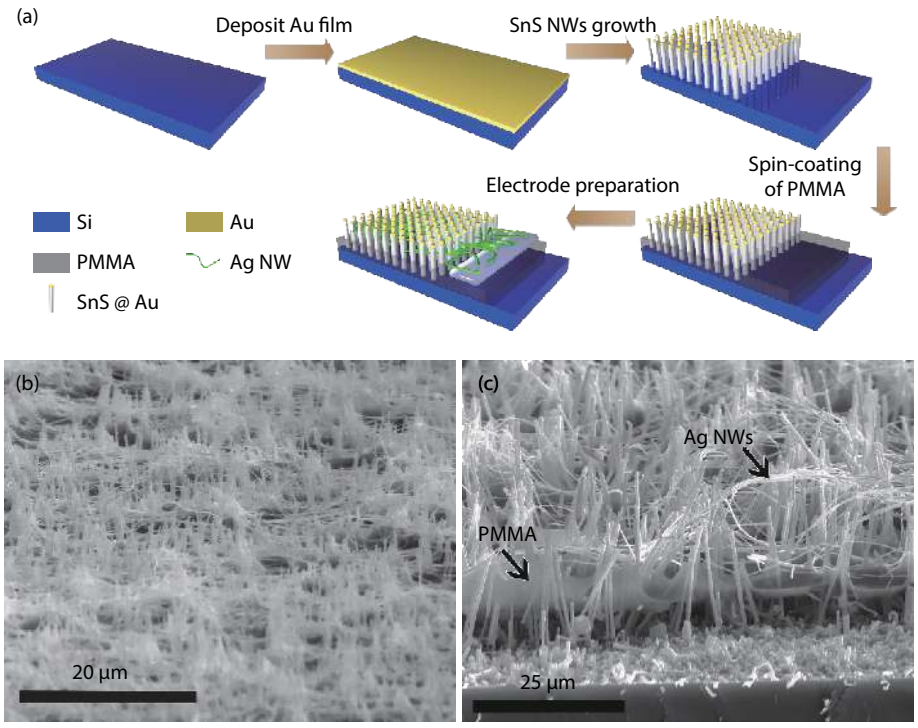

Fig. 3. (Color online) (a) Schematic of the fabrication process of the aligned SnS nanowire arrays based photodetectors. (b) SEM images of the aligned SnS nanowires deposited with PMMA and Ag nanowires.

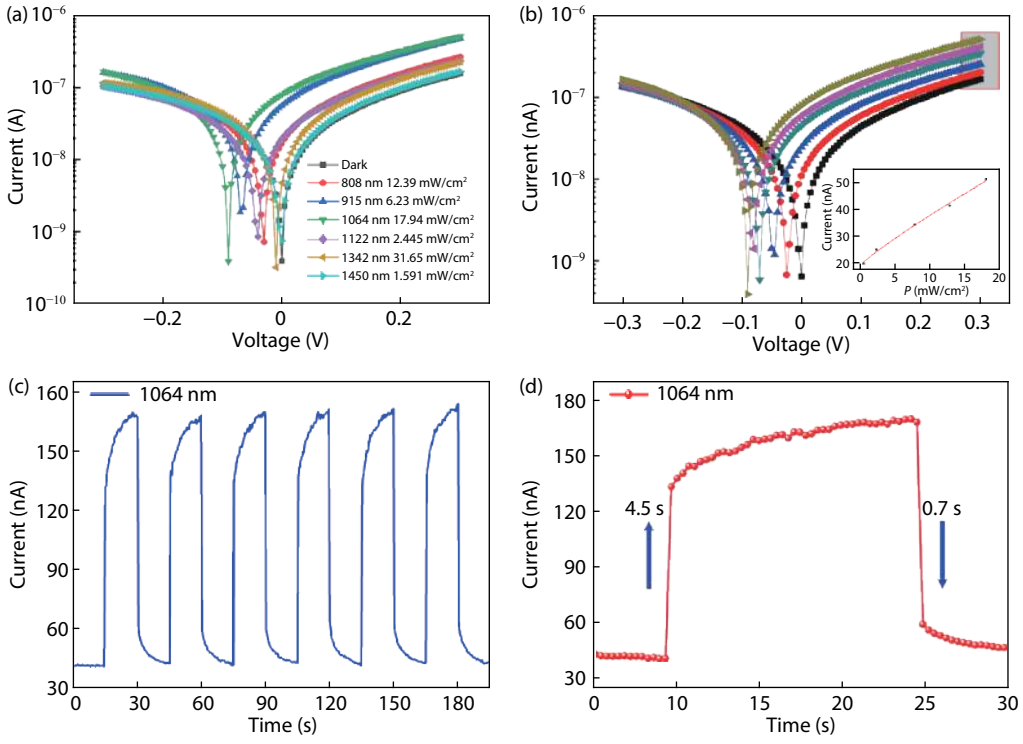

Fig. 4. (Color online) Characterizations of the aligned SnS nanowire array based photodetectors. (a) *I*–*V* curves of the nanowire array device to NIR lights with different wavelengths. (b) *I*–*V* curves of the device to 1064 nm lights with different light intensities. (c) Reproducible and stable switching behavior of the device to 1064 nm light. (d) Transient response and decay time of the device.

The photoresponse performance of the aligned NW arrays based photodetectors were then measured at room temperature. Fig. 4(a) gave the *I*–*V* curves of the device to NIR lights with different wavelengths as well as in dark condition. Similar to single SnS NW, the NW arrays based photodetectors exhibited obvious response to NIR lights with light wavelengths ranging from 808 to 1450 nm. As the direct bandgap of SnS is 1.1 eV, we then studied the photoresponse of the SnS NW arrays based photodetector to the NIR light with the wavelength of 1064 nm in detail. Photoresponse of the device to 1064 nm light with different light intensities was shown in Fig. 4(b). The photocurrents were

found increased gradually with increased light intensities and their relationship was plotted as $\Delta I \sim 2.38 \times P^{0.89}$ (Fig. 4(b) inset). For photodetectors, stability is one of the key factors for their practical applications. The repeatability and response speed of the NW arrays based devices were thus studied. Fig. 4(c) depicted the dynamic current-time curves of the device to 1064 nm light at a fixed light intensity of (17.94 mW/cm^2). It was found that, under same conditions, both the photocurrent and the I_{on}/I_{off} ratio of the aligned SnS NW arrays based device were largely improved compared with those of single SnS NW based device, indicating the improvement of light absorbing ability of the NW arrays[11–13]. Besides, with periodically turning the incident light on and off for cycles, no visible change of the photocurrents was found for the device, confirming the excellent reproducibility and stability. The response time and the recovery time of the device can be deduced from the dynamic *I*–*T* curve shown in Fig. 4(d), which was calculated to be about 4.5 and 0.7 s, respectively. These results indicated that the as-fabricated array device had a favorable photoresponse properties compared with other state-of-the-art infrared photodetectors based on semiconductor nanowires reported in the literature[7, 30–32].

4. Conclusion

In conclusion, we successfully synthesized aligned SnS NW arrays via a simple chemical vapor deposition method. As-growth NWs exhibited excellent response to near infrared lights in terms of good responsivity, high external quantum efficiency and fast response time. Photodetectors were built on the aligned SnS NW arrays. Due to the light trapping ability of the aligned NW arrays, both the photocurrent and the I_{on}/I_{off} ratio of the aligned SnS NW arrays based device were largely improved compared with their single SnS NW counterpart. By using direct transfer method, flexible photodetectors are expected to be fabricated for next generation flexible electronic applications and related work is still in progress.

Acknowledgements

This work was financial supported by National Natural Science Foundation of China (61625404, 61888102).

References

[1] Steinmann V, Jaramillo R, Hartman K, et al. 3.88% efficient tin sulfide solar cells using congruent thermal evaporation. Adv Mater, 2014, 26, 7488
[2] Zhao L, Tan G, Hao S, et al. Ultrahigh power factor and thermoelectric performance in hole-doped single-crystal SnSe. Science, 2016, 351, 141
[3] Rath T, Gury L, Sanchez-Molina I, et al. Formation of porous SnS nanoplate networks from solution and their application in hybrid solar cells. Chem Commun, 2015, 51, 10198
[4] Kumar G M, Fu X, Ilanchezhiyan P, et al. Highly sensitive flexible photodetectors based on self-assembled tin monosulfide nanoflakes with graphene electrodes. ACS Appl Mater Interface, 2017, 9(37), 32142
[5] Lin Y, Wen X, Wang L, et al. Structure and optical properties of SnS nanowire arrays prepared with two-step method. Adv Mater Res, 2012, 476, 1519
[6] Zhou X, Gan L, Zhang Q, et al. High performance near-infrared photodetectors based on ultrathin SnS nanobelts grown via physical vapor deposition. J Mater Chem C, 2016, 4(11), 2111
[7] Zheng D, Fang H, Long M, et al. High-performance near-infrared photodetectors based on p-type SnX (X = S, Se) nanowires grown via chemical vapor deposition. ACS Nano, 2018, 12(7), 7239
[8] Chao J, Wang Z, Xu X, et al. Tin sulfide nanoribbons as high performance photoelectrochemical cells, flexible photodetectors and visible-light-driven photocatalysts. RSC Adv, 2013, 3, 2746
[9] Zhang Z, Yang J, Zhang K, et al. Anisotropic photoresponse of layered 2D SnS-based near infrared photodetectors. J Mater Chem C, 2017, 5(43), 11288
[10] Deng Z, Cao D, He J, et al. Solution synthesis of ultrathin single-crystalline SnS nanoribbons for photodetectors via phase transition and surface processing. ACS Nano, 2012, 6, 6197
[11] Ning L, Jiang T, Shao Z, et al. Light-trapping enhanced ZnO-MoS_2 core-shell nanopillar arrays for broadband ultraviolet-visible-near infrared photodetection. J Mater Chem C, 2018, 6, 7077
[12] Zhang D, Gu L, Zhang Q, et al. Increasing photoluminescence quantum yield by nanophotonic design of quantum-confined halide perovskite nanowire arrays. Nano Lett, 2019, 19(5), 2850
[13] Gu L, Tavakoli M M, Zhang D, et al. 3D arrays of 1024-pixel image sensors based on lead halide perovskite nanowires. Adv Mater, 2016, 28, 9713
[14] Fan Z, Kapadia R, Leu P, et al. Ordered arrays of dual-diameter nanopillars for maximized optical absorption. Nano Lett, 2010, 10, 3823
[15] Fan Z, Razzavi H, Do J, et al. Three-dimensional nanopillar-array photovoltaics on low-cost and flexible substrate. Nat Mater, 2009, 8, 648
[16] Duan X, Lieber C M. General synthesis of compound semiconductor nanowires. Adv Mater, 2000, 12, 298
[17] Wu Y, Yang P. Direct observation of vapor-liquid-solid nanowire growth. J Am Chem Soc, 2001, 123, 3165
[18] Shen G, Xu J, Wang X, et al. Growth of directly transferrable In_2O_3 nanowire mats for transparent thin-film transistors applications. Adv Mater, 2011, 23, 771
[19] Luo T, Liang B, Liu Z, et al. Single-GaSb-nanowire-based room temperature photodetectors with broad spectral response. Sci Bull, 2015, 60, 101
[20] Duan T, Lou Z, Shen G. Electrical transport and photoresponse properties of single-crystalline Cd_3As_2 nanowires. Sci China-Phys Mech Astron, 2015, 58, 027801
[21] Li L, Lou Z, Shen G. Flexible broadband image sensors with SnS quantum dots/Zn_2SnO_4 nanowires hybrid nanostructures. Adv Funct Mater, 2018, 18, 1705389
[22] Chen S, Lou Z, Chen D, et al. Printble Zn_2GeO_4 microwires based flexible photodetectors with tunable photorespone. Adv Mater Technol, 2018, 3, 1800050
[23] Lou Z, Li L, Shen G. $InGaO_3$(ZnO) superlattice nanowires for high performance ultraviolet photodetectors. Adv Electron Mater, 2015, 1, 1500054
[24] Lou Z, Yang X L, Chen H R, et al. Flexible ultraviolet photodetectors based on ZnO–SnO_2 heterojunction nanowire arrays. J Semicond, 2018, 39(2), 024002
[25] Chen G, Liang B, Liu X, et al. High-performance hybrid phenyl-C61-butyric acid methyl ester/Cd_3P_2 nanowire ultraviolet-visible-near infrared photodetectors. ACS Nano, 2014, 8, 787
[26] Lou Z, Li L, Shen G. Ultraviolet/visible photodetectors with ultrafast, high photosensitivity based on 1D ZnS/CdS heterostructures. Nanoscale, 2016, 8, 5219
[27] Chai R, Lou Z, Shen G. Highly flexible self-powered photodetectors based on core-shell Sb/CdS nanowires. J Mater Chem C, 2019, 7, 4581
[28] Liu Z, Luo T, Liang B, et al. High-detectivity InAs nanowire photodetectors with spectral response from ultraviolet to near-infrared. Nano Res, 2013, 6, 775
[29] Gong X, Tong M, Xia Y, et al. High-detectivity polymer photodetect-

ors with spectral response from 300 nm to 1450 nm. Science, 2009, 325, 1665

[30] Miao J, Hu W, Guo N, et al. Single InAs nanowire room temperature near-infrared photodetectors. ACS Nano, 2014, 8, 3628

[31] Ouyang B, Zhang K, Yang Y, et al. Photocurrent polarity controlled by light wavelength in self-powered ZnO nanowires/SnS photodetector system. iScience, 2018, 1, 16

[32] Chen G, Liang B, Liu Z, et al. High performance rigid and flexible visible-light photodetectors based on aligned X(In,Ga)P nanowire arrays. J Mater Chem C, 2014, 2, 1270